Stabilization of Monodomain Polarization in Ultrathin $PbTiO_3$ Films

D. D. Fong,[1] A. M. Kolpak,[2] J. A. Eastman,[1] S. K. Streiffer,[1] P. H. Fuoss,[1] G. B. Stephenson,[1] Carol Thompson,[3] D. M. Kim,[4] K. J. Choi,[4] C. B. Eom,[4] I. Grinberg,[2] and A. M. Rappe[2]

[1]*Materials Science Division, Argonne National Laboratory, Argonne, Illinois 60439, USA*
[2]*The Makineni Theoretical Laboratories, Department of Chemistry, University of Pennsylvania, Philadelphia, Pennsylvania 19104, USA*
[3]*Department of Physics, Northern Illinois University, DeKalb, Illinois 60115, USA*
[4]*Department of Materials Science and Engineering, University of Wisconsin, Madison, Wisconsin 53706, USA*

(Received 22 September 2005; published 28 March 2006)

Using *in situ* high-resolution synchrotron x-ray scattering, the Curie temperature T_C has been determined for ultrathin *c*-axis epitaxial $PbTiO_3$ films on conducting substrates ($SrRuO_3$ on $SrTiO_3$), with surfaces exposed to a controlled vapor environment. The suppression of T_C was relatively small, even for the thinnest film (1.2 nm). We observe that 180° stripe domains do not form, indicating that the depolarizing field is compensated by free charge at both interfaces. This is confirmed by *ab initio* calculations that find polar ground states in the presence of ionic adsorbates.

DOI: 10.1103/PhysRevLett.96.127601 PACS numbers: 77.80.−e, 64.70.Nd, 68.55.−a, 77.84.Dy

One of the outstanding fundamental questions for ferroelectric thin films is understanding the stability of the polar phase when the polarization has a component perpendicular to the film plane. Although such orientations are desired for many applications [1] and can be obtained (e.g., by compressive epitaxial strain [2]), the polarization change at the film boundaries creates a ''depolarizing field'' that must be neutralized for the polar phase to be stable [3]. Two mechanisms are available to reduce the depolarizing field energy: compensation by free charge at the boundaries [4] or the formation of equilibrium stripe domains with oppositely oriented polarization [5]. In both cases, the trade-off between bulk energy gain and surface energy cost leads to a suppression of the phase transition to the polar phase as films become thinner. These fundamental size effects may dramatically alter behavior in ultrathin films.

Here we focus on stabilization of the single-domain state in ultrathin ferroelectric perovskite films by interfacial charge. Key issues are determining the critical thickness, below which the monodomain, perpendicularly polarized state is not stable, and understanding the nature of the interfacial charge compensation. Previous experimental studies of ultrathin epitaxial films on conductive substrates have been carried out using electrical measurements [6], piezoresponse force microscopy (PFM) [7,8], and x-ray lattice parameter measurements [8]. These studies have found stable monodomain ferroelectricity at room temperature in films as thin as 3–4 nm. Lattice parameter measurements indicated a 50% reduction in $PbTiO_3$ polarization when film thickness was reduced to 3 nm [8], which was explained using a model based on the finite screening length for charge in conducting electrodes [4]. Interestingly, in some of these studies [7,8], the film did not have an electrode on the exposed surface. This suggests that interface compensation adequate to stabilize ultrathin polar films can occur by a mechanism other than electronic conduction, e.g., by the accumulation of charged ions [9]. For relatively thick ferroelectric films exposed to ambient atmosphere, there is strong experimental evidence for surface compensation by ionic adsorption [7,10–12]. Furthermore, monodomain ferroelectric films have been observed on nonconducting substrates [13–15], and it has been proposed that high-mobility electrons can exist at heterointerfaces in perovskite insulators due to unusual bonding states [16]. The adequacy of these alternative, ''chemical'' rather than ''electronic'' mechanisms for reducing depolarization field energy sufficiently to stabilize ultrathin polar films is relatively unexplored.

In this Letter, we report a joint experimental and theoretical study of the paraelectric-ferroelectric phase transition in ultrathin $PbTiO_3$ films grown on conducting substrates, with surfaces exposed to a controlled vapor environment. The structures of films as thin as 1.2 nm (3 unit cells) were determined as a function of temperature (T) using high-resolution grazing-incidence x-ray scattering. The polar phase was observed to form and remain single domain for all thicknesses studied (1.2–9.2 nm). The observed stability of the monodomain phase is explained by *ab initio* calculations that find a polar ground state if ionic adsorbates are present on the surface. The polarization direction is predicted to depend on the chemical nature of the adsorbate.

The conducting substrates were epitaxial $SrRuO_3$ films grown on $SrTiO_3(001)$ single crystals by pulsed laser deposition [17]. The $PbTiO_3$ films were grown by metal-organic chemical vapor deposition (MOCVD) under conditions described previously [18]. Grazing-incidence synchrotron x-ray scattering was used for *in situ* monitoring of the film during epitaxial growth and for subsequent observation of the phase transition as a function of T [14]. This method allows study at high T while maintaining film

stoichiometry and a well-controlled vapor interface and the study of ferroelectricity in films too thin to be characterized by other methods. Four $PbTiO_3$ films of different thickness were studied: Three of the films (1.2, 2.0, and 3.6 nm) were grown at 930 K on 10-nm-thick $SrRuO_3$ layers; the thickest $PbTiO_3$ film (9.2 nm) was grown at 990 K on a 50-nm-thick $SrRuO_3$ layer. All of the layers replicated the high crystalline quality of the substrates (0.01° typical mosaic) and were measured to be fully lattice matched to the underlying $SrTiO_3$. This compressive epitaxial strain produces polarization perpendicular to the film plane [2].

X-ray experiments were carried out at beam line 12ID-D of the Advanced Photon Source, as described previously [14]. The Curie temperature T_C was determined by measuring the T dependence of the c (out-of-plane) lattice parameter. Figure 1 shows measurements along the 30L crystal truncation rod (CTR) for a 9.2 nm- (23 unit-cell-) thick $PbTiO_3$ film at various temperatures. This region of the CTR extends through the 304 peaks of $PbTiO_3$, $SrRuO_3$, and $SrTiO_3$. From the position of the $PbTiO_3$ peak, one can see that c increases as the film polarizes below T_C, because of the strong polarization-strain coupling in this system [2]. The many fringes observed from the thicknesses of the $SrRuO_3$ and $PbTiO_3$ layers indicate the high quality of the interfaces.

For the 9.2 nm film, we also performed *ex situ* room-T PFM. We were able to ''write'' inverted domains by applying a positive voltage to the tip and to determine that the as-grown state of the film was a single domain having a polarization directed out of the film (''up'' polarization). For all films, we searched *in situ* near T_C for satellites in the diffuse x-ray scattering around the $PbTiO_3$ Bragg peaks, which occur when equilibrium 180° stripe domains are present [5,14]. None were observed, indicating that all the films transform directly into the monodomain polar state.

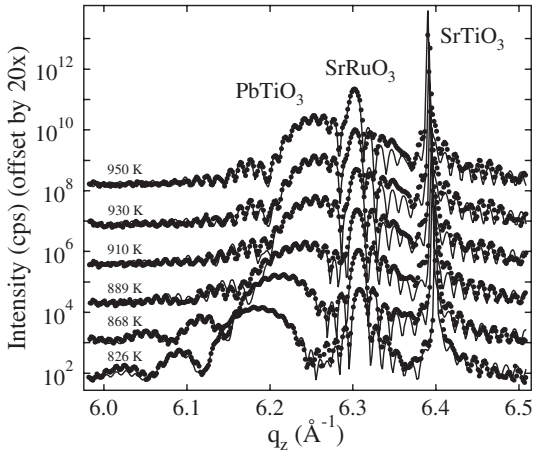

FIG. 1. X-ray scattering intensity along the 30L CTR, showing the 304 Bragg peaks and finite-thickness fringes from 9.2-nm-thick $PbTiO_3$ and 50-nm-thick $SrRuO_3$ films at various temperatures. The shift of the $PbTiO_3$ peak to lower q_z upon cooling indicates an expansion of the c lattice parameter.

Values for the $PbTiO_3$ lattice parameter c as a function of T were determined by fitting the x-ray CTR data to a 3-layer model (two films and a substrate) [13]. For the fits shown here, we assumed that the $PbTiO_3$ polarization direction is up, with the square of atom displacements proportional to the change in c from its $P = 0$ value, and that the $SrRuO_3$ is SrO terminated [19] and the $PbTiO_3$ is PbO terminated [20]. Changing these assumptions does not significantly affect the results for c. For each sample, the numbers of $PbTiO_3$ and $SrRuO_3$ unit cells were fixed. Eight parameters were varied in the fitting procedure: lattice constants, layer roughnesses, and interface offsets for the $SrRuO_3$ and $PbTiO_3$ layers, a scale factor for the $SrRuO_3$, and an overall scale factor for the total scattered intensity. This simple structural model is able to reproduce the CTR intensities very well for all thicknesses and temperatures. Typical best fits are shown with the data in Fig. 1.

Figure 2 shows the dependence of c on T for each film thickness, as well as the predicted T dependence of c for thick, coherently strained $PbTiO_3$ lattice-matched to $SrTiO_3$ [2,14]. In the thick limit, the (second order) nonpolar to polar transition is located at $T_C^\infty = 1025$ K, as indicated by the abrupt change in slope. We extracted T_C for each film by estimating the temperature at which the slope of $c(T)$ changed, as shown by the solid lines in Fig. 2. The theoretical slope was used above T_C. Since we have no data above T_C for the 3.6 nm film, that estimate of T_C is a lower bound.

These results stand in some contrast to recently reported room-T lattice parameters of $PbTiO_3$ films on Nb-doped $SrTiO_3$ substrates [8], which showed a decrease in c for thinner films. We see no change in c as a function of thickness at our lowest T (550 K), even for smaller thicknesses than previously measured, although there is a clear variation in T_C with thickness. Note also that we observe a systematic change in c with thickness in the nonpolar

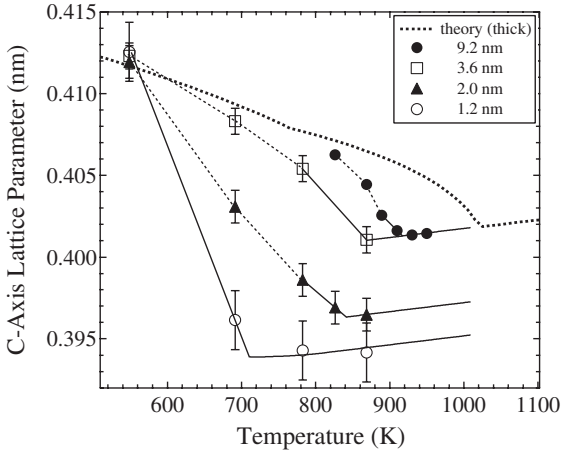

FIG. 2. The c lattice parameter vs T for each film, with solid lines showing the break in slope used to estimate T_C. The upper curve is the Landau theory prediction for thick $PbTiO_3$ on $SrTiO_3$ [2].

phase. Caution should thus be used when relating c to polarization or T_C suppression in ultrathin films using measurements at only one T.

The values of T_C as a function of film thickness are shown in Fig. 3. Also shown are values of T_C for $PbTiO_3$ grown directly on insulating $SrTiO_3$, in which 180° stripe domains have formed [5]. In both cases, T_C increases towards the calculated T_C^∞ for thick films and decreases by hundreds of degrees below this limit for ultrathin films. The transition temperatures for $PbTiO_3$ on $SrRuO_3$ are somewhat higher than those on $SrTiO_3$, in agreement with the observed difference in the equilibrium domain morphology: The conducting $SrRuO_3$ electrode lowers the energy of the single-domain state, producing a direct transition from unpolarized to monodomain polarized at a higher T_C. The dependence of $T_C^\infty - T_C$ on film thickness we observe does not obey the power law predicted by the simplest theories of screening in electrodes [21] but, instead, appears to be similar to that previously seen for films on insulating substrates.

The observation that polarization occurs without formation of 180° domains implies that both the top and bottom interfaces of these films must be almost completely compensated by free charge [3]. Thus, a $SrRuO_3$ electrode will compensate $PbTiO_3$ with a voltage offset small enough that even a 3-unit-cell-thick film polarizes above room temperature. This is in agreement with recent *ab initio* calculations on films with two $SrRuO_3$ electrodes [22]. The behavior of the top surface is perhaps even more intriguing—although there is no conductor to supply electronic charge, exposure to the ambient vapor of the MOCVD growth environment evidently supplies sufficient free charge from ions to neutralize the depolarizing field.

To quantitatively verify whether adsorbed ions can stabilize the polar state in ultrathin films, we have performed *ab initio* density functional theory (DFT) calculations on the structure and energetics of $PbTiO_3$ films on $SrRuO_3$ bottom electrodes with various molecules adsorbed to the surface. Based on the composition of the MOCVD environment, we chose to study H, O, OH, H_2O, and CO_2 adsorption. Calculations were performed using methods described previously [22,23]. We modeled 3-unit-cell-(1.2-nm-) thick $PbTiO_3$ films supported by 3 unit cells of $SrRuO_3$, with a SrO-TiO_2 interface between $PbTiO_3$ and $SrRuO_3$ and a PbO terminated $PbTiO_3$ surface. A vacuum of >2 nm separated periodic copies of the structures in the direction perpendicular to the surface, and a dipole correction was included in the center of the vacuum region to remove the artificial electric field due to the asymmetry in ''electrode'' materials. The in-plane lattice constant was fixed to the calculated zero-stress a value for bulk $PbTiO_3$, which approximates the effect of the $SrTiO_3$ substrate in the experiments. Data are reported for films with one adsorbate on a single unit-cell surface area; modeling of the $c(2 \times 2)$ surface showed that the experimentally and theoretically determined reconstruction [20,24] was present both with and without adsorbates but did not significantly affect the energy difference between the bare and adsorbed states.

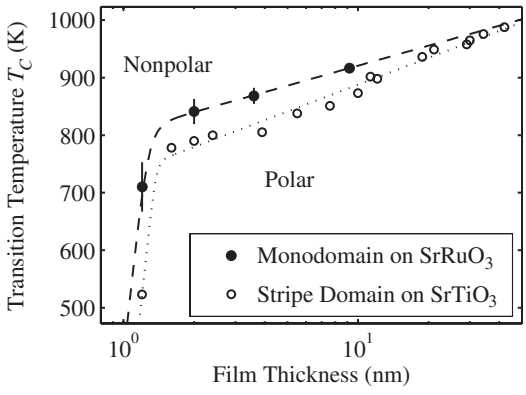

FIG. 3. $PbTiO_3$ T_C vs film thickness for monodomain films on conducting $SrRuO_3$ (this work) and stripe-domain films on insulating $SrTiO_3$ (previous work [5]). Curves are guides to the eye.

For a bare surface, the ground state of the ferroelectric film was found to be nonpolar. With OH, O, or H adsorbates present, however, the ground state was polar, with atoms displaced from the centrosymmetric positions. Table I gives values of polarization relative to the theoretical bulk value $P_{\text{bulk}} = 0.75\ \text{C/m}^2$, calculated from the average over all PbO and TiO_2 layers of the cation-anion displacements $\Delta z = z_{\text{cation}} - z_{\text{O}}$, each divided by the corresponding Δz in bulk theoretical $PbTiO_3$. Since the conductive $SrRuO_3$ electrode can provide either positive or negative compensation charge, the chemical nature of the adsorbate determines the direction of polarization. An overlayer of OH or O, which bind to the surface Pb, enforces an upwards polarization, while an overlayer of H, which bind to the surface O, stabilizes polarization in the opposite direction. On the other hand, CO_2 adsorption gives a very weak polarization, and undissociated H_2O molecules bind only weakly to the surface, preserving the nonpolar state.

Table I also shows the differences in energy ΔE_{DFT} between the film with bound adsorbate and the separated bare film and free adsorbate atom (or OH molecule). To compare these $T = 0$ K energies to experimental conditions, we estimated the standard Gibbs free energy of adsorption $\Delta G^0(T) = \Delta H^0(T) - T\Delta S^0(T)$. The change in enthalpy ΔH^0 is estimated from ΔE_{DFT} by adding $P\Delta V \approx -k_B T$. A small correction for zero-point energy

TABLE I. Polarization and ΔE_{DFT} from DFT calculations, with estimated reaction energies per adsorbate at $T = 300$ K.

Adsorbate	$P/\lvert P_{\text{bulk}}\rvert$	ΔE_{DFT} (eV)	ΔH^0 (eV)	ΔG^0 (eV)	ΔG (eV)
OH	0.7	−2.00	−2.34	−1.96	−0.20
O	0.9	−0.92	−0.95	−0.52	1.95
H	−0.8	−2.90	−2.93	−2.65	0.79

and spin polarization is also applied for the case of OH adsorption. The change in entropy ΔS^0 is primarily due to the differences between the bound and free adsorbates. We estimated the entropy of the bound adsorbates [25] and used tabulated entropies for free OH, O, and H at 1 bar [26]. Values of ΔG^0 at $T = 300$ K are given in Table I. The free energy change under experimental conditions is $\Delta G = \Delta G^0 - k_B T \ln p_{\text{exp}}$, where p_{exp} is the adsorbate partial pressure. For these experiments, the partial pressure of O_2 was controlled at 3.3×10^{-3} bar, while that of H_2O varied between 2×10^{-6} and 1×10^{-9} bar depending upon the reactions of the MOCVD process gases. To obtain the values of ΔG in Table I, the partial pressures of free O, H, and OH at $T = 300$ K were calculated using $p_{H_2O} = 5 \times 10^{-7}$ bar [26]. Inspection of these ΔG values shows that only OH adsorption is thermodynamically favored in our experimental environment.

The thermodynamic stability of OH adsorbates implies that the stable monodomain polarization direction is up, in agreement with the PFM result. The simple thermodynamic estimate presented here suggests that the full coverage of OH would desorb from the 3-unit-cell-thick film above $T = 450$ K, resulting in a nonpolar film. Preliminary calculations that allow for partial coverage of OH give a higher transition T, in closer agreement with the observed $T_C = 700$ K.

Our DFT calculations verify that surface charge passivation by OH adsorbates is indeed adequate to stabilize the observed monodomain state in these films. For ultrathin films, the chemisorption energy of 2 eV is much larger than the bulk free energy difference between the polar and nonpolar states at zero field (e.g., 0.2 eV per unit-cell area for a 3-unit-cell-thick film). Such a strong influence of interfacial chemistry on polarization has broad implications for ultrathin ferroelectric films. To understand polarization stability, it will be necessary for measurements to be performed with controlled interfacial chemistry. The behavior of ferroelectric films with exposed surfaces [7,8,10–12] may differ significantly from those sandwiched between two electrodes [4,6,22]. In the former case (e.g., PFM experiments), the switching mechanism likely involves a change in adsorbate. Charged impurities at buried interfaces may play a similar chemical role to the surface-adsorbed ions considered here. Exploitation of these effects for novel devices or templating techniques may be possible, both through chemical control of polarity and through polarization control of ionic adsorption.

Work supported by the U.S. Department of Energy, Office of Science, Basic Energy Sciences under Contract No. W-31-109-ENG-38. A. M. K. was supported by Arkema, Inc. C. B. E. acknowledges support from NSF DMR-0313764 and ECS-0210449. A. M. R. acknowledges support from the ONR N00014-00-1-0372 and N00014-01-1-0365 and the AFOSR FA9550-04-1-0077. Computational support was provided by the DoD through the HPCMO and an NSF CRIF grant.

[1] R. Ramesh and D. G. Schlom, Science **296**, 1975 (2002).
[2] N. A. Pertsev and V. G. Koukhar, Phys. Rev. Lett. **84**, 3722 (2000).
[3] I. Kornev, H. Fu, and L. Bellaiche, Phys. Rev. Lett. **93**, 196104 (2004).
[4] J. Junquera and Ph. Ghosez, Nature (London) **422**, 506 (2003).
[5] D. D. Fong, G. B. Stephenson, S. K. Streiffer, J. A. Eastman, O. Auciello, P. H. Fuoss, and Carol Thompson, Science **304**, 1650 (2004).
[6] V. Nagarajan *et al.*, Appl. Phys. Lett. **84**, 5225 (2004).
[7] T. Tybell, C. H. Ahn, and J.-M. Triscone, Appl. Phys. Lett. **75**, 856 (1999).
[8] C. Lichtensteiger, J.-M. Triscone, J. Junquera, and Ph. Ghosez, Phys. Rev. Lett. **94**, 047603 (2005).
[9] O. Dulub, U. Diebold, and G. Kresse, Phys. Rev. Lett. **90**, 016102 (2003).
[10] S. V. Kalinin and D. A. Bonnell, Phys. Rev. B **63**, 125411 (2001).
[11] S. V. Kalinin, C. Y. Johnson, and D. A. Bonnell, J. Appl. Phys. **91**, 3816 (2002).
[12] F. Peter, K. Szot, R. Waser, B. Reichenberg, S. Tiedke, and J. Szade, Appl. Phys. Lett. **85**, 2896 (2004).
[13] Carol Thompson, C. M. Foster, J. A. Eastman, and G. B. Stephenson, Appl. Phys. Lett. **71**, 3516 (1997).
[14] S. K. Streiffer, J. A. Eastman, D. D. Fong, Carol Thompson, A. Munkholm, M. V. Ramana Murty, O. Auciello, G.-R. Bai, and G. B. Stephenson, Phys. Rev. Lett. **89**, 067601 (2002).
[15] D. D. Fong *et al.*, Phys. Rev. B **71**, 144112 (2005).
[16] A. Ohtomo and H. Y. Hwang, Nature (London) **427**, 423 (2004).
[17] J. Choi, C. B. Eom, G. Rijnders, H. Rogalla, and D. H. A. Blank, Appl. Phys. Lett. **79**, 1447 (2001).
[18] M. V. Ramana Murty, S. K. Streiffer, G. B. Stephenson, J. A. Eastman, G.-R. Bai, A. Munkholm, O. Auciello, and Carol Thompson, Appl. Phys. Lett. **80**, 1809 (2002).
[19] G. Rijnders, D. H. A. Blank, J. Choi, and C. B. Eom, Appl. Phys. Lett. **84**, 505 (2004).
[20] A. Munkholm, S. K. Streiffer, M. V. Ramana Murty, J. A. Eastman, Carol Thompson, O. Auciello, L. Thompson, J. F. Moore, and G. B. Stephenson, Phys. Rev. Lett. **88**, 016101 (2002).
[21] I. P. Batra, P. Wurfel, and B. D. Silverman, J. Vac. Sci. Technol. **10**, 687 (1973).
[22] Na Sai, A. M. Kolpak, and A. M. Rappe, Phys. Rev. B **72**, 020101(R) (2005).
[23] We used DFT with the generalized gradient approximation as implemented in the *ab initio* code DACAPO, with ultrasoft pseudopotentials generated with the VASP code, a plane wave cutoff of 400 eV, a $4 \times 4 \times 1$ Monkhorst-Pack k-point mesh, and an fast-Fourier-transform grid of 8 points/Å in all 3 directions.
[24] C. Bungaro and K. M. Rabe, Phys. Rev. B **71**, 035420 (2005).
[25] For O and H, we used $3k_B$. For OH, a more accurate estimate based on DFT vibrational frequencies gave 6–$12k_B$ for $T = 200$–1000 K.
[26] Values online at http://webbook.nist.gov/chemistry.